Res Chem Intermed
https://doi.org/10.1007/s11164-018-3404-2

Liquid-phase oxidation of toluene to benzaldehyde with molecular oxygen catalyzed by copper nanoparticles supported on graphene

Guangliang Song[1] · **Liang Feng**[1] · **Jie Xu**[1] · **Hongjun Zhu**[1]

Received: 3 October 2017 / Accepted: 19 March 2018

Abstract Highly-dispersed copper nanoparticles (Cu NPs) were fabricated on the surface of reduced graphene oxide via direct hydrazine hydrate reduction of Cu^{2+} in aqueous solution. Scanning electron microscope and transmission electron microscope images show that the Cu NPs are distributed on the surface of graphene nanosheets, and the average particle size was about 40 nm. The Cu NPs supported on graphene have high reaction activity for the oxidation of toluene to corresponding benzaldehyde. It was found that the selectivity reached 66.5% and the conversion of toluene reached 11.5%.

Keywords Copper nanoparticles · Graphene · Toluene oxidation

Introduction

Graphene, a kind of two-dimensional single layer material with sp^2 hybridized carbons, exhibits excellent properties in various areas, which span from energy storage, diode and nanophotonic devices to supporters of nanocatalysts [1–6]. Particularly in catalytic research, graphene, which has a large specific surface, has been extensively studied as a support for the dispersion of other materials [7–13].

Recently, extensive researches have reported that graphene–inorganic nanomaterial-based hybrid materials have been applied in different catalytic systems

---

✉ Guangliang Song
songgl@njtech.edu.cn

✉ Hongjun Zhu
zhuhj@njtech.edu.cn

[1] Department of Applied Chemistry, College of Chemistry and Molecular Engineering, Nanjing Tech University, Nanjing 211816, China

[14–16]. Incorporating metal nanoparticles into graphene has recently attracted significant interest.

For example, noble metal nanoparticles (NPs) such as Pd and Pt supported on graphene have been used as s catalyst for oxidation reduction reaction (ORR) [17, 18]. However, Cu NPs synthesized by chemical reduction of copper salts with hydrazine hydrate in solution show prominent advantages such as simplicity and feasibility [19–21].

On the other hand, the oxidation of toluene is one of the most important functional group transformations in organic synthesis because of its oxidation products, benzaldehyde (BzH), benzyl alcohol (BzOH) and benzoic acid (BzA). Generally, gas-phase and liquid-phase oxidation can achieve oxidation of toluene. It is well known that gas-phase oxidation need high temperatures and high pressure [22]. Compared with gas-phase oxidation, liquid-phase oxidation provides catalytic oxidation processing under relatively mild conditions [23, 24]. BzH, a typical product of toluene oxidation, is a very important material for the synthesis of spices and pharmaceutical intermediates, dyestuffs and the agrochemical industries. Generally, in industry, BzH is produced by the hydrolysis of benzylidene chloride [25]. However, chlorine unavoidably exists in the product, limiting the use of the BzH. Therefore, overcoming this problem has prompted research on the liquid-phase oxidation of toluene to BzH [26]. In the process of toluene oxidation, it is harder to obtain BzH than BzOH and BzA. So, many researchers have tried many different catalysts in the oxidation of toluene including MnO_x, porphyrin, Ag/WO_3 and so on [24, 27, 28]. Copper-containing carbon nitride polymer ($Cu–C_3N_4$) was synthesized by Zhang [29], and used as a catalyst in the liquid-phase oxidation of toluene with 18.3% conversation. However, the total selectivity of BzOH, BzH and BzA was only 79.4% under optimum conditions. Han [30] reported a novel Cu- and boron-doped graphitic carbon nitride catalyst (Cu–CNB) for the selective oxidation of toluene to BzH, but used tert-butyl hydroperoxide as the oxidant. However, there has so far been no report on toluene oxidation catalyzed over Cu/graphene. Also, Cu NPs exhibit excellent catalytic performance in ORR as already stated. Therefore, they is very significant for the study of toluene oxidation over Cu/graphene.

Here, we have tried toluene catalytic oxidation by Cu NPs supported on graphene. Cu NPs supported on graphene with good catalytic activity and high selectivity for toluene oxidation to BzH were achieved.

Experimental

Instruments and materials

Chemicals used in this study including toluene (A.R.), graphite powder and cupric sulfate were provided by Shanghai Linfeng Chemical. H_2O_2 (30%) and hydrazine hydrate were obtained from Nanjing Chemical Reagent. The standard benzyl alcohol, benzaldehyde and benzoic acid were purchased from Wuxi Yasheng Chemical. HPLC analysis ($H_2O:CH_3CN = 65:35$, $v = 1$ mL/min, $\lambda = 254$ nm) was performed on a DIONEX HPLC-2004 equipped with a C18 column and a UV–VIS detector. The supported Cu NPs were characterized by transmission electron microscopy (TEM) (JEOL 2010 LaB6) and scanning electron microscopy (SEM) (Hitachi S-3400 N). The XRD of the samples was characterized on a Bruker-D8 Advance X-ray diffractometer with Cu Kα radiation.

Synthesis of graphene oxide (GO)

A modified Hummer's method [31] was used to prepare graphene oxide (GO) and reduced graphene (RGO). A total of 2.0 g of graphite powder and 46 mL of H_2SO_4 (98%) were placed in a flask and stirred for 2 h. Then, $KMnO_4$ (10.0 g) was added slowly into the flask while the temperature was maintained at 273 K. The mixture was then transferred into a water bath, which was maintained at 308 K for 30 min. Finally, deionized (DI) water was added continuously into the flask under vigorous stirring. The temperature was increased to 363 K and maintained for another 30 min. Next, 6.0 mL H_2O_2 (30%) was added into the mixture to end the reaction, and the color of solution turned light yellow immediately. The mixture was filtered with a PP Millipore filter (pore size = 0.22 μm), and then washed with DI water three times and ethanol three times. The filter was then dissolved in 2 L DI water to acquire 1 mg/mL GO solution.

Synthesis of Cu/graphene

The GO solution (1.0 mg/mL) and the $CuSO_4$ solution (0.1 mol/L) were mixed at a volume ratio (200:4 mL). After stirring for 10 h, 30 mL of KOH solution (1 mol/L) and 4 mL of hydrazine hydrate (80 wt%) solution were added into the mixture. Then, 100 mg cetyl trimethyl ammonium bromide (CTAB) was slowly added into the mixture to prevent the agglomeration of the nanoparticles. The mixture were placed in a water bath at 353 K for 2 h to accomplish the reduction of both GO and Cu^{2+}. Finally, the system was filtered to remove the reducing agents and washed with DI water and ethanol several times. The filter was dried in a vacuum at 338 K.

Synthesis of Cu NPs

Amounts of 4 mL $CuSO_4$ solution (0.1 mol/L) and 30 mL KOH solution (1 mol/L) were placed in a flask, then 4 mL of hydrazine hydrate (80 wt%) solution and 100 mg CTAB were slowly added into the mixture. The mixture was placed in a water bath at 353 K for 2 h to accomplish the reduction of Cu^{2+}. Finally, the system was filtered to remove the reducing agents and washed with DI water and ethanol several times. The filter was dried in a vacuum at 338 K.

Toluene oxidation over Cu/graphene

Amounts of 12.0 g toluene, 0.6 g catalyst, 6 mL 30% H_2O_2 and solvent 150 mL methanol were added to a 500-mL autoclave with a mechanical stirrer which was charged with oxygen to maintain a pressure of 2.0 MPa. The system was stirred at the reaction temperature for 11 h. At the end of the reaction, the mixture solution was filtered to remove the catalyst. The yield was analyzed by HPLC [32] and nitrobenzene as the internal standard.

Characterization

SEM (INSPECT-F; FEI) was used to analyze the metal nanoparticles supported on grapheme film. The crystalline phases of the prepared films were measured by thin-film X-ray diffraction (XRD; X'pert pro-MPD). The microstructure of the prepared films was measured using TEM (JEM-2100F; JEOL, Japan). The contents of BzH, BzOH and BzA were characterized by HPLC.

Results and discussion

Characterizations of the catalyst

Figure 1 illustrates the XRD patterns of Cu/graphene as compared with that of graphene. The XRD spectrum of Cu/graphene (Cu loading 9.6%) showed characteristic peaks at 43.1°, 50.5°, and 74.9° [33] with very high intensity. These peaks were assigned to the (110), (200) and (220) crystallographic planes of the cubic copper crystal in the XRD patterns of Cu/graphene, respectively. The crystallite sizes of the Cu/graphene and graphene were 36.1 nm and 35.9 nm, respectively, according to the Scherrer equation. Figure 2 shows the TEM and SEM images of the Cu/graphene nanostructure. The SEM micrograph shows the surface morphology of the Cu/graphene films and reveals that the Cu NPs were either distributed on the surface of graphene sheets or covered by the graphene sheets, which was confirmed by the XRD conclusions. Meanwhile, the TEM image reveals

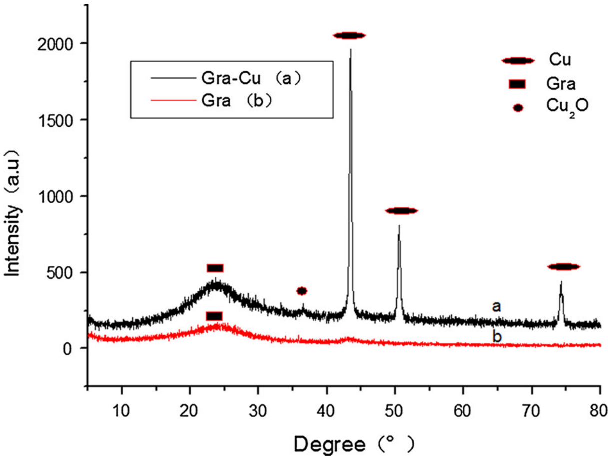

Fig. 1 XRD spectrum of Cu/graphene and graphene films

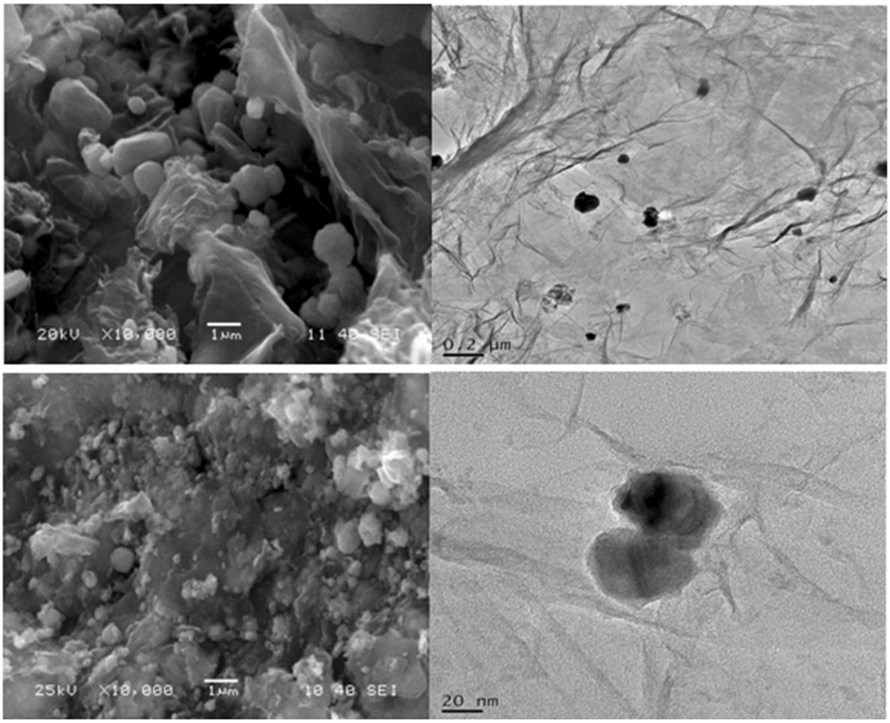

Fig. 2 SEM of Cu/graphene films (*left*) and TEM of Cu/graphene films (*right*)

that Cu NPs were wrapped in graphene sheets and the average size of the Cu NPs was about 40 nm.

Conversion and selectivity of toluene oxidation by Cu/graphene

The toluene oxidation conversion and selectivity catalyzed by Cu NPs, Cu/graphene, graphene and blank tests at 8 h, 338 K and 2.0 MPa O_2, respectively, are listed in Table 1. Graphene itself had little activity in toluene oxidation [34] which was even below the blank tests in toluene catalytic oxidation. And Cu NPs

Table 1 Catalytic performance over various catalysts in toluene oxidation

Entries	Catalyst	Conv (%)	BzOH (%)	BzH (%)	BzA (%)
1	None	0.21	32.6	62.7	4.6
2	Copper	4.1	32.3	52.4	15.2
3	Graphene	0.2	23.4	71.0	5.5
4	Cu/graphene	11.5	11.0	66.5	22.5

Reaction conditions: toluene 12.0 g, catalyst 0.6 g, methanol 150 mL, reaction temperature 338 K, reaction time 8 h and pressure 2.0 MPa had higher conversion (4.1%). Interestingly, the toluene conversion was significantly improved to 11.5% by Cu/graphene. The high reaction activity could be contributing to the highly-dispersed distribution of the Cu NPs on the graphene surface. Furthermore, the selectivity of BzH reached 66.5% in the toluene oxidation which was much higher than BzA (22.5%) and BzOH (11.0%).

The change of toluene oxidation conversion and selectivity with the reaction process are shown in Fig. 3a. As the reaction proceeded from 1 to 11 h, the selectivity of the BzH decreased continuously with the selectivity of BzA increasing and the selectivity of BzOH remaining almost unchanged. These results indicated that the generating rate of BzH was slower than its conversion to BzA from 1 to 11 h. The conversion of toluene increased continuously from 1 to 11 h. Additionally, there was an increase in the yield of BzH from 1 to 8 h, and a decrease in the yield of BzH after 8 h. The highest yield reached 7.25% at 8 h.

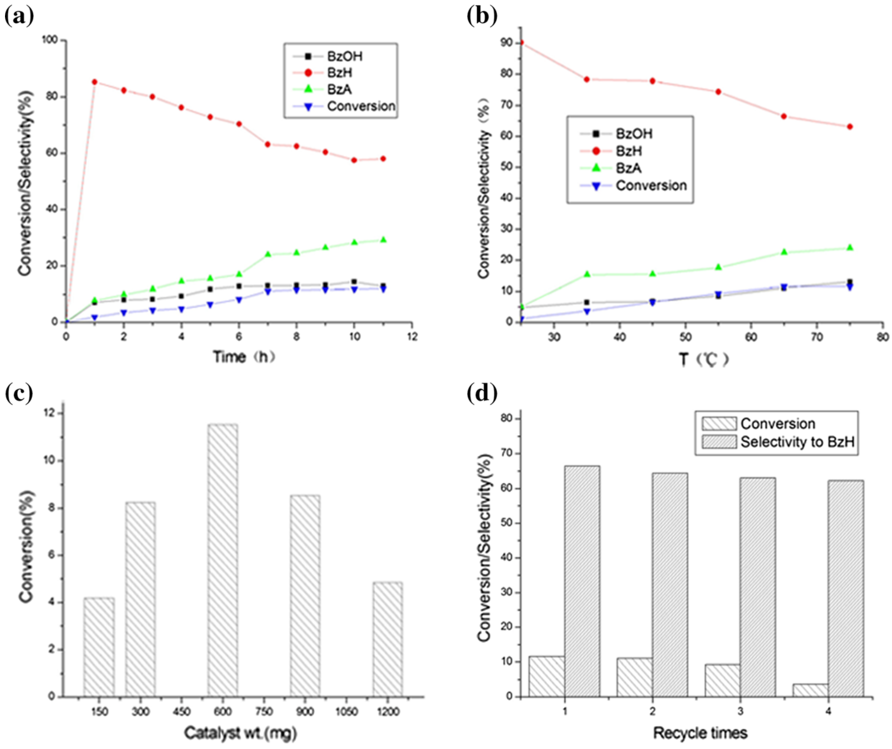

Fig. 3 **a** The conversion and selectivity of toluene with reaction time. Reaction conditions: toluene 12.0 g, 9.6 wt% Cu/graphene 0.6 g, methanol 150 mL, reaction temperature 338 K, pressure 2.0 MPa. **b** The conversion and selectivity at various reaction temperatures. Reaction conditions: toluene 12.0 g, reaction time 8 h, methanol 150 mL, catalyst 0.6 g and pressure 2.0 MPa. **c** The conversion of toluene with different weight of catalyst. Reaction conditions: toluene 12.0 g, reaction temperature 338 K, reaction time 8 h, methanol 150 mL, pressure 2.0 MPa. **d** The reusability of the catalyst. Reaction conditions: substrate/metal mass ratio 20, reaction temperature 338 K, reaction time 8 h and pressure 2.0 MPa

The effect of reaction temperature on the catalytic performance is shown in Fig. 3b. The conversion of toluene increased from 1.2 to 11.5% with an increase of the reaction temperature from 298 to 348 K at 8 h, but the selectivity of BzH decreased, and meanwhile the selectivity of BzOH and BzA increased as the temperature increased. This implies that, as the reaction temperature rose, the generating rate of BzH was slower than that of its conversion into BzA. Both conversion and selectivity were considered, and st 338 K, the optimum temperature, the conversion of toluene reached 11.5% and the selectivity of BzH reached 66.5%.

Furthermore, the effect of catalyst weight on the catalytic performance is shown in Fig. 3c. The results show that the conversion of toluene increased from 4.2 to 11.5% as the catalyst weight increased from 150 mg to 600 mg, whereas, when the catalyst weight exceeded 600 mg, the conversion decreased continuously.

Effect of O_2 pressures and solvents

The effect of O_2 pressures and solvents are shown in Tables 2 and 3. As shown in Table 2, the conversation of toluene increased from 0.5 to 12.2% as the O_2 pressure was increased from 0.5 to 2.5 Mpa. And when the O_2 pressure was increased from 0.5 to 2.0 Mpa, the relative contents of BzA increased from 4.7 to 22.5% and BzH decreased from 82.7 to 66.5%, while the BzOH showed almost no change. But when the O_2 pressure increased from 2.0 to 2.5 Mpa, the relative contents of BzH rapidly reduced from 66.5 to 52.2% while BzA increased from 22.5 to 38.6%. This fact can be explained partly because the BzH converts easily to BzA at high pressure.

As shown in Table 3, the conversation of toluene was increased from 5.6% in a weak polar solvent such as CH_3CN to 8.2% in a strong polar solvent such as CH_3COOH, and then to 11.2% in a medium polar solvent such as CH_3OH. And in CH_3COOH, the main oxidation product of toluene was BzOH, which was confirmed by previous research [35]. In weak polar solvents such as CH_2Cl_2 and CH_3CN, the BzH was 42.6 and 50.4%, respectively, while in a medium polar solvent such as CH_3OH BzH it was 66.5%.

Table 2 Effect of O_2 reaction pressures

Entries	O_2 (Mpa)	Conv (%)	BzOH (%)	BzH (%)	BzA (%)
1	0.5	0.5	12.6	82.7	4.7
2	1.0	2.3	12.3	74.0	15.7
3	1.5	5.6	11.9	68.8	19.3
4	2.0	11.5	11.0	66.5	22.5
5	2.5	12.2	11.2	50.2	38.6

Reaction conditions: toluene 12.0 g, catalyst 0.6 g, methanol 150 mL, reaction temperature 338 K, reaction time 8 h

Table 3 Affection of solvents

Entries	Solvents	Conv (%)	BzOH (%)	BzH (%)	BzA (%)
1	CH_3COOH	8.2	78.2	12.7	9.1
2	CH_2Cl_2	6.7	35.8	42.6	21.6
3	CH_3CN	5.6	35.2	50.4	14.4
4	CH_3OH	11.5	11.0	66.5	22.5

Reaction conditions: toluene 12.0 g, catalyst 0.6 g, solvent 150 mL, reaction temperature 338 K, reaction time 8 h and pressure 2.0 MPa

Reusability of the catalyst

After the reaction finished, the reused catalyst was obtained by centrifuging, washing several times by ethanol, and drying at 338 K in a vacuum for 4 h. This catalyst was used in the next run under the same conditions and the results are shown in Fig. 3d. In the first three times, there is no significant decrease in the conversion from 11.5 to 9.3% and selectivity from 66.5 to 63.1%, and the activity of the catalyst was almost unchanged. Unfortunately, the toluene conversion declined to 3.7% at the fourth time likely attributed to the decrease in the amount of Cu NPs. Moreover, the XRD patterns of fresh and reused Cu/graphene (Fig. 4) were almost unchanged, which suggested that the structure and the composition of the reused catalyst were also unchanged. These results imply that the catalyst could be separated and recycled.

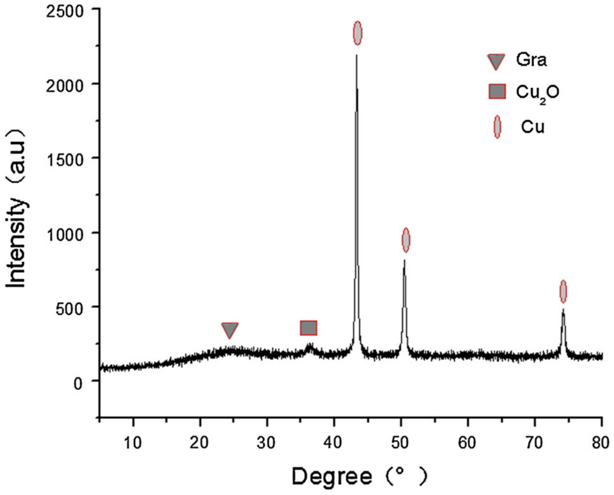

Fig. 4 XRD spectrum of the reused Cu/graphene films after 4 times

Conclusions

In this study, we have found that highly-dispersed Cu NPs could be supported on the surface of RGO via a direct hydrazine hydrate reduction of Cu^{2+} in aqueous solution. The complex catalyst Cu/graphene (9.6%) used in toluene oxidation with oxygen as oxidant exhibited excellent conversion of toluene (11.5%) and selectivity to BzH (66.5%). Furthermore, this catalyst shows excellent conversion and selectivity without changing its catalytic activity even after 3 reuses.

Acknowledgements This work is financially supported by the National key R&D Program of China (2017YFB0307202), the Industry-Academy-Research Prospective joint project of Jiangsu Province (BY2016005-06) and Jiangsu Planned Projects for Postdoctoral Research Funds (1402213C).

References

1. Y. Zhu, S. Murali, W. Cai, X. Li, J.W. Suk, J.R. Potts, R.S. Ruoff, Adv. Mater. **22**, 3906 (2010)
2. M. Lee, K. Lee, S. Kim, H. Lee, J. Park, K. Choi, H. Kim, D. Kim, D. Lee, S. Nam, J. Park, Nano Lett. **13**, 2814 (2013)
3. S. Oh, T.G. Kim, S. Kim, Y. Jo, S.S. Lee, K. Kim, B. Ryu, J. Park, Y. Choi, S. Jeong, Chem. Mater. **28**, 4714 (2016)
4. H. Lee, T.K. Choi, Y.B. Lee, H.R. Cho, R. Ghaffari, L. Wang, H.J. Choi, T.D. Chung, N. Lu, T. Hyeon, S.H. Choi, D. Kim, Nat. Nanotech. **11**, 566 (2016)
5. S. Lee, A. Reuveny, J. Reeder, S. Lee, H. Jin, Q. Liu, T. Yokota, T. Sekitani, T. Isoyama, Y. Abe, Z. Suo, T. Someya, Nat. Nanotech. **11**, 472 (2016)
6. Y. Jo, J.Y. Kim, S. Kim, Y. Seo, K. Jang, S.Y. Lee, S. Jung, B. Ryu, H. Kim, J. Park, Y. Choi, S. Jeong, Nanoscale **9**, 5072 (2017)
7. Y. Li, W. Gao, L. Ci, C. Wang, P.M. Ajayan, Carbon **48**, 1124 (2010)
8. D.R. Dreyer, H.P. Jia, C.W. Bielawski, Angew. Chem. Int. Ed. Eng. **49**, 6813 (2010)
9. X. Wang, P.F. Fulvio, G.A. Baker, G.M. Veith, R.R. Unocic, S.M. Mahurin, M. Chi, S. Dai, Chem. Commun. **46**, 4487 (2010)
10. G.M. Scheuermann, L. Rumi, P. Steurer, W. Bannwarth, R. Mulhaupt, J. Am. Chem. Soc. **131**, 8262 (2009)
11. S. Guo, S. Dong, Chem. Soc. Rev. **40**, 2644 (2011)
12. Y. Zhang, L. Zhang, C. Zhou, Acc. Chem. Res. **46**, 2329 (2013)
13. D.C. Marcano, D.V. Kosynkin, J.M. Berlin, A. Sinitskii, Z. Sun, A. Slesarev, L.B. Alemany, W. Lu, J.M. Tour, ACS Nano **4**, 4806 (2010)
14. K.H. Lee, S. Han, K. Kwon, J.B. Park, J. Colloids Interfaces Sci. **403**, 127 (2013)
15. N. Shang, C. Feng, H. Zhang, S. Gao, R. Tang, C. Wang, Z. Wang, Catal. Commun. **40**, 111 (2013)
16. R. Nie, J. Wang, L. Wang, Y. Qin, P. Chen, Z. Hou, Carbon **50**, 586 (2012)
17. J. Shi, R. Nie, P. Chen, Z. Hou, Catal. Commun. **41**, 101 (2013)
18. K. Szori, R. Puskas, G. Szollosi, I. Bertoti, J. Szepvoelgyi, M. Bartok, Catal. Lett. **143**, 539 (2013)
19. J. Hwang, T. Yoon, S.H. Jin, J. Lee, T. Kim, S.H. Hong, S. Jeon, Adv. Mater. **25**, 6724 (2013)
20. C.O. Ania, M. Seredych, E. Rodriguez-Castellon, T.J. Bandosz, Appl. Catal. B Environ. **163**, 424 (2015)
21. A.S. Nia, S. Rana, D. Doehler, X. Noirfalise, A. Belfiore, W.H. Binder, Chem. Commun. **50**, 15374 (2014)
22. S. Xie, H. Dai, J. Deng, Y. Liu, H. Yang, Y. Jiang, W. Tan, A. Ao, G. Guo, Nanoscale **5**, 11207 (2013)
23. M. Ilyas, M. Sadiq, Catal. Lett. **128**, 337 (2009)
24. G. Huang, J. Luo, C.C. Deng, Y.A. Guo, S.K. Zhao, H. Zhou, S. Wei, Appl. Catal. A Gen. **338**, 83 (2008)
25. K.T.V. Rao, P.S.N. Rao, R. Nagaraju, P.S.S. Prasad, N. Lingaiah, J. Mol. Catal. A Chem. **303**, 84 (2009)
26. F. Wang, J. Xu, X.Q. Li, J. Gao, L.P. Zhou, R. Ohnishi, Adv. Synth. Catal. **347**, 1987 (2005)

27. X.Q. Li, J. Xu, F. Wang, J. Gao, L.P. Zhou, G.Y. Yang, Catal. Lett. **108**, 137 (2006)
28. S. Ghosh, S.S. Acharyya, D. Tripathi, R. Bal, J. Mater. Chem. A **2**, 15726 (2014)
29. F. Zhang, J. Li, Guangdong. Chem. Eng **12**, 127 (2017)
30. H. Han, G. Ding, T. Wu, D. Yang, T. Jiang, B. Han, Molecules **20**, 12686 (2015)
31. N. Cao, Y. Zhang, J. Nanomater. **2015**, 168125 (2015)
32. A. Dubey, B.G. Mishra, Catal. Commun. **8**, 1507 (2007)
33. L. Jiang, X. Lu, X. Zheng, J. Mater. Sci. Mater. **25**, 174 (2014)
34. Y. Li, X. Huang, Y. Li, Y. Xu, Y. Wang, E. Zhu, X. Duan, Y. Huang, Sci. Rep. **3**, 1549 (2013)
35. J. Ma, J. Yu, W. Chen, A. Zeng, Catal. Lett. **146**, 1600 (2016)